

See discussions, stats, and author profiles for this publication at: <https://www.researchgate.net/publication/40678332>

Evaporation-Induced Crystallization of Pluronic F127 Studied in Situ by Time-Resolved Infrared Spectroscopy

ARTICLE in THE JOURNAL OF PHYSICAL CHEMISTRY A · DECEMBER 2009

Impact Factor: 2.69 · DOI: 10.1021/jp908162z · Source: PubMed

CITATIONS

25

READS

40

4 AUTHORS:



[Plinio Innocenzi](#)

Università degli Studi di Sassari

211 PUBLICATIONS 4,813 CITATIONS

[SEE PROFILE](#)



[Luca Malfatti](#)

Università degli Studi di Sassari

107 PUBLICATIONS 1,367 CITATIONS

[SEE PROFILE](#)



[Massimo Piccinini](#)

ENEA

155 PUBLICATIONS 1,545 CITATIONS

[SEE PROFILE](#)



[Augusto Marcelli](#)

INFN - Istituto Nazionale di Fisica Nucleare

394 PUBLICATIONS 3,989 CITATIONS

[SEE PROFILE](#)

Evaporation-Induced Crystallization of Pluronic F127 Studied in Situ by Time-Resolved Infrared Spectroscopy

Plinio Innocenzi* and **Luca Malfatti**

Laboratorio di Scienza dei Materiali e Nanotecnologie, D.A.P., Università di Sassari, and CR-INSTM, Palazzo del Pou Salid, Piazza Duomo 6, 07041 Alghero (Sassari), Italy

Massimo Piccinini

Porto Conte Ricerche S.r.l., SP 55 Porto Conte/Capo Caccia km 8, 400, 07041 Alghero (SS), Italy

Augusto Marcelli

Laboratori Nazionali di Frascati—INFN, Via E. Fermi 40, 00044, Frascati, Italy

Received: August 24, 2009; Revised Manuscript Received: November 05, 2009

Rapid scan time-resolved infrared spectroscopy has been used to study *in situ* the crystallization induced by evaporation in an aqueous solution of a triblock copolymer, Pluronic F127. A droplet of the solution was cast on a silicon substrate and the evaporation followed by an infrared microscope in transmission mode. The evaporation rate of water, in the last stage of the process, has been shown to be correlated to the changes in the block copolymer; four different stages can be distinguished. The block copolymer passes from an amorphous micellar state in water to a partially crystallized phase in well-defined stages of the evaporation; the complete change from amorphous to crystalline state of Pluronic F127 is observed only after all water is evaporated.

Introduction

Amphiphilic block copolymers of the poly(ethylene oxide)-*b*-poly(propylene oxide)-*b*-poly(ethylene oxide) (PEO-PPO-PEO) family¹ have recently known a booming interest because their self-assembly capability has found important applications in nanoscience; an example is their use as templates for mesoporous materials.² PEO-PPO-PEO copolymers associate in aqueous solutions to form micelles which basically consist of a PPO core and a corona with hydrated PEO segments.³ This property has been widely exploited to expand the applications of block copolymers from traditional application areas such detergents, adhesives, additives, and lubricants to the field of nanoscience and nanotechnology.^{4,5} Block copolymer derived nanoporous materials are nowadays an important topic of research, and their ability of self-assembly into nanometer-sized structures such as lamellae, cylinders, spheres, and gyroids is used as a tool to generate mesoporous materials with a controlled and ordered porosity. The process of formation of mesostructured oxide and hybrid organic–inorganic thin films templated by a surfactant micelle has been named as evaporation-induced self-assembly (EISA).⁶ Evaporation of the solvent drives the self-assembly by a complex balance of the different phenomena that are simultaneously involved during self-organization;⁷ mesostructural order through evaporation is achieved if the kinetics of the processes involved follow a well-defined hierarchy.⁸ Several experimental techniques have been applied to follow *in situ* the self-assembly process, and small-angle X-ray scattering (SAXS),⁹ in particular, has been shown to be a powerful tool to obtain time-resolved information about the organization process induced by EISA in thin films. Another important analytical technique is infrared spectroscopy that can also be used *in situ* to follow EISA¹⁰ and can be coupled to

SAXS for simultaneous analysis.¹¹ Time-resolved infrared spectroscopy is one of the few techniques that allow following *in situ* the chemical–physical processes behind evaporation phenomena.¹² In a series of previous works, we have developed and applied this technique to EISA of mesostructured thin films¹³ and to simple systems, such as water¹⁴ and ethanol,¹⁵ to elucidate the fundamental processes during evaporation. In the present article we have extended the application of rapid scan infrared spectroscopy to study *in situ* the evaporation of a droplet of aqueous solution containing a triblock copolymer, Pluronic F127. This method allows monitoring how the evaporation of water drives the phase changes of the block copolymer at the different stages of the process.

Experimental Section

A solution of a triblock copolymer, Pluronic F127 ($\text{EO}_{106}\text{PO}_{70}\text{EO}_{106}$, EO = ethylene oxide and PO = propylene oxide), in water, 5 wt %, was prepared using bidistilled water. Pluronic F127 was purchased by Aldrich and used as received; (100) oriented, P-type/boron doped silicon wafers were purchased by Jocam and used as the substrates.

Time-resolved *in situ* infrared (IR) analysis was performed using a Bruker Vertex 70 interferometer equipped with a Globar source. The IR measurements were performed in the range $600\text{--}7000\text{ cm}^{-1}$ with a resolution of 8 cm^{-1} . A MCT detector ($250 \times 250\text{ }\mu\text{m}$ size) cooled to the liquid nitrogen temperature and a KBr beamsplitter were used. To study the evaporation of a cast droplet of Pluronic F127 in water, Rapid-scan time-resolved (RSTR) measurements were performed by averaging four interferograms per spectrum in an acquisition time of 0.8 s and a time interval of 2 s between the beginning of the acquisition of consecutive spectra. We have selected the scan time to optimize the signal-to-noise ratio and resolution as a function of the experimental conditions.

* Corresponding author.

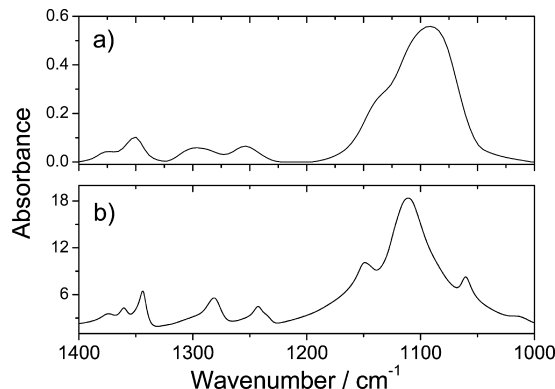


Figure 1. FTIR absorption spectra in the 1400–1000 cm^{−1} range of Pluronic F127 in 5 wt % aqueous solution (a) and in the solid state (b).

The relative humidity (RH %) during the experiment was carefully monitored, and a closed cabinet was mounted around the microscope to control the RH, which was kept constant at 45%. The measurements were performed at 25 °C and at ambient pressure.

A Bruker Hyperion 3000 IR microscope working in transmission mode and a one side polished silicon wafer as substrate were used; the background spectrum of the Si substrate was recorded as the average of 128 interferograms. A small drop of water–Pluronic F127 mixture (~1 μL) was cast on the silicon substrate; the measurement was started immediately afterward. Another experimental parameter that we have optimized is the droplet size. Indeed, if the drop is too big, the signal in the middle-IR range will be saturated for most of the measurement time; on the other hand small droplets show a very fast evaporation and are not suitable for time-resolved studies with a conventional source. We have followed the evaporation of the droplet during several runs to ensure the reproducibility of the experimental conditions. Reference spectra of Pluronic F127 in the solid state have been obtained using a KBr pellet. The results were analyzed by Bruker Opus 6.5 Software; curve fitting was obtained using the Levenberg–Marquadt method and Gaussian curves; the quality of the fit was evaluated by the residual error (rms).

Images of the water–Pluronic F127 after evaporation were recorded by mapping the sample using the CCD camera installed in the microscope.

The wide-angle X-ray diffraction pattern of the F127 droplet cast on silicon wafer was recorded by a Bruker D8 diffractometer with an X-ray generator working at a power of 40 kV and 40 mA. The Cu K α radiation ($\lambda = 1.5418 \text{ \AA}$) was used to perform $\omega/2\theta$ scans in an angular range from 10° to 70° with angle step size of 0.05° and 10 s of exposition time per step.

Small-angle X-ray scattering (SAXS) patterns were collected by a Rigaku “Micro-Max 3000” equipped with a pinhole SAXS camera design. The system uses a high-brilliance X-ray source working at 20 kV and 20 mA collimating in conjunction with pinholes and position-sensitive detectors. The sample to detector distance and the instrumental grazing angle between X-ray beam and sample were set at 1400 cm and 2.2°, respectively. Cu K α radiation ($\lambda = 1.5418 \text{ \AA}$) was used to collect the diffraction pattern by a 2D multiwire proportional counter (1024 × 1024 pixels). The final plot was obtained by radial integration of the 2D pattern.

Results and Discussion

Amorphous and Crystalline Pluronic F127 Infrared Spectra. The infrared spectra of Pluronic F127 in the amorphous and crystalline states exhibit very distinctive features that allow distinguishing quite well between the two phases; these states

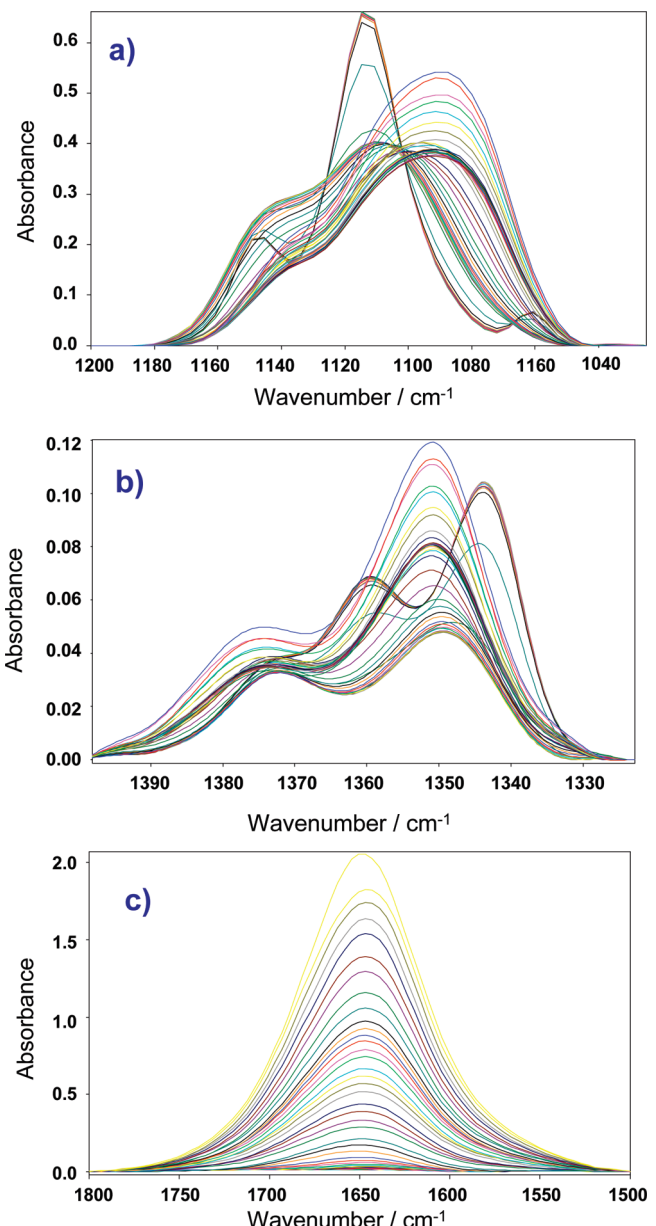


Figure 2. FTIR absorption spectra recorded by rapid scan time-resolved IR spectroscopy and referred to the last 120 s of the evaporation process in the 1200–1020 (a), 1400–1310 (b), and 1800–1500 cm^{−1} ranges (c). Colors in the spectra are used as a guide for eyes.

have been characterized and the thermal induced transition between amorphous and crystalline block copolymer has been widely investigated.^{16–18} Figure 1 shows the FTIR absorption spectra in the 1400–1000 cm^{−1} range of Pluronic F127 in a 5 wt % aqueous solution (Figure 1a) and in the solid state (Figure 1b). We report the two spectra to give a specific assignment of the bands that we have used to monitor the evaporation-induced crystallization of Pluronic F127 in water as a function of time.

The FTIR spectrum of crystalline Pluronic F127¹⁹ is characterized, in the C–O–C stretching region (~1200–1000 cm^{−1}), by a typical triplet of intense overlapped bands at 1060 ($\nu_s(\text{COC}) + \rho_s(\text{CH}_2)$), 1111 ($\nu_s(\text{COC})$ or $\nu_{as}(\text{COC})$), and 1150 ($\nu(\text{CC}) - \nu_{as}(\text{COC})$) cm^{−1}. These bands undergo a significant change when Pluronic F127 is dissolved in water and is in the amorphous state; in fact, only one broad intense band peaking around 1111 cm^{−1} with a shoulder around 1150 cm^{−1} is observed while the peak at 1063 cm^{−1}, which is distinctive of the helical structure of PEO in the crystalline state,²⁰ disappears.

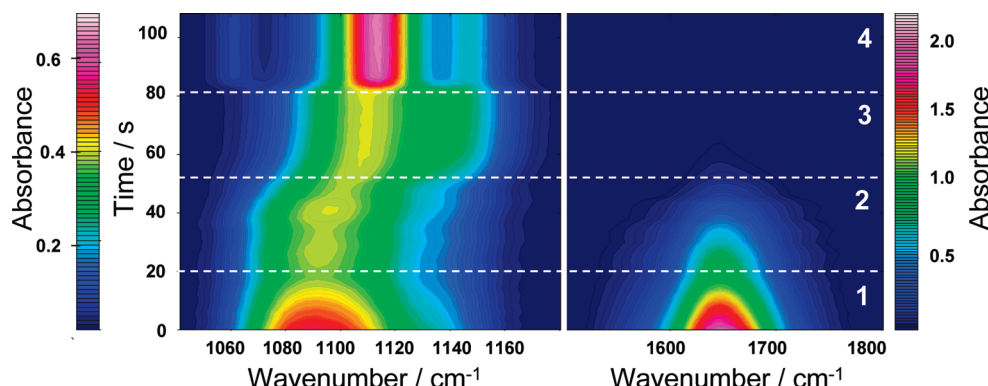


Figure 3. 3D time-resolved infrared spectra of an evaporating droplet of Pluronic–water in the 1040–1180 (left) and 1500–1800 cm⁻¹ ranges (right). Numbers from 1 to 4 indicate the different evaporation stages, for details refers to the text.

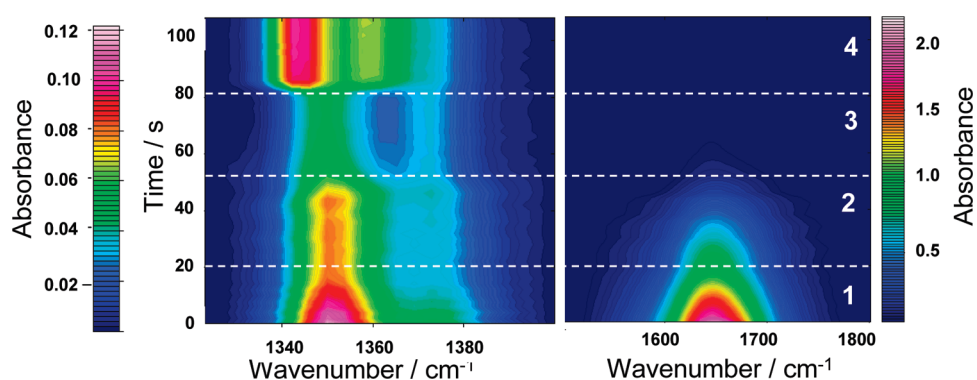


Figure 4. 3D time-resolved infrared spectra of an evaporating droplet of Pluronic–water in the 1320–1400 (left) and 1500–1800 cm⁻¹ ranges (right). Numbers from 1 to 4 indicate the different evaporation stages, for details refer to the text.

The C–O–C stretching mode at 1111 cm⁻¹ is quite sensitive to hydrogen bonding between water and the oxygens in the block copolymer,²¹ and when Pluronic F127 is dissolved in water, this band shifts to lower wavenumbers and broadens. This indicates that the PEO-PPO-PEO molecules in the aqueous environment have a higher mobility and a disordered packing with respect to the solid state.

In the CH₂ twisting region (~1200–1320 cm⁻¹) the crystalline Pluronic F127 shows three specific bands of weaker intensity at 1236 cm⁻¹ ($t_{as}(\text{CH}_2)$ – $t_s(\text{CH}_2)$), helix structure (shoulder), 1244 cm⁻¹ ($t_s(\text{CH}_2)$) and 1280 ($t_{as}(\text{CH}_2)$ + $t_s(\text{CH}_2)$) cm⁻¹, trans structure; also these bands broaden and shift to higher wavenumbers in the spectra of the amorphous state (Figure 1a).

In the wagging region (~1400–1320 cm⁻¹) the spectrum of crystalline Pluronic F127 (Figure 1b) shows another two bands at 1344 ($w_{as}(\text{CH}_2)$) and 1360 ($w_s(\text{CH}_2)$ + $\nu(\text{CC})$) cm⁻¹, which, as the twisting bands, broaden and shift to higher wavenumbers in the amorphous state. The decrease in intensity of these two bands is accompanied by a corresponding increase in intensity of a band at 1350 cm⁻¹, which is recognized as a distinctive feature of the amorphous phase.²² The spectra show also another band at 1376 cm⁻¹ assigned to the CH₃ deformation mode, which is generally reported to be sensitive to the chemical environment and to intermolecular interactions.²³

Time-Resolved Study of an Evaporating Water–Pluronic F127 Droplet. We have used a rapid scan time-resolved FTIR technique to study *in situ* the evaporation of a droplet of water–Pluronic F127 solution. We have chosen a concentration of 5% by weight at 25 °C of block copolymer; following the phase diagram in these conditions the surfactant forms an isotropic solution.²⁴ We have optimized the water droplet dimension to be able to obtain a good reproducibility of the

phenomenon, a good signal-to-noise ratio, and to avoid saturation of the infrared bands during the measure. The overall evaporation of the droplet takes several minutes, but we have focused our attention on the last 3–4 min of the process which are the most significant for the phenomenon. The time resolution limit of the technique is in the millisecond scale, but for our process a time scale of seconds is a suitable temporal resolution. Figure 2, shows the sequence of spectra, in selected ranges, recorded by RSTR in the last 120 s of the droplet evaporation. The different spectra are shown in colors as a guide for eyes to allow a better identification; these spectra have been used to draw the 3D images that allow getting a direct visualization of the different stages of the phenomenon during evaporation (vide infra, Figures 3 and 4). We have selected these specific ranges because they show the C–O–C stretching region (Figure 2a, 1200–1030 cm⁻¹) and the wagging region (Figure 2b, 1400–1320 cm⁻¹) whose bands undergo specific changes between the amorphous and the crystalline state; we have also monitored the water evaporation by RSTR using the water bending mode at 1650 cm⁻¹ (Figure 2c, 1800–1500 cm⁻¹). The spectra in the wagging and stretching regions show significant changes with evaporation time; simultaneously the water band exhibits a continuous decrease in intensity until the completion of the process. We have reproduced these results in 3D graphs which allow a direct visualization; we have coupled, in the Figures 3 and 4, the 3D representation of the spectra in the bending and wagging region with that of water, to obtain an immediate correlation between water evaporation and block copolymer phase transitions. Figure 3 (left side) shows the three-dimensional (3D) time-resolved infrared spectra with the time evolution of the bands in the C–O–C stretching region (1180–1040 cm⁻¹); on the right side the 3D RSTR spectra of water in the bending region are shown. The x-axis represents

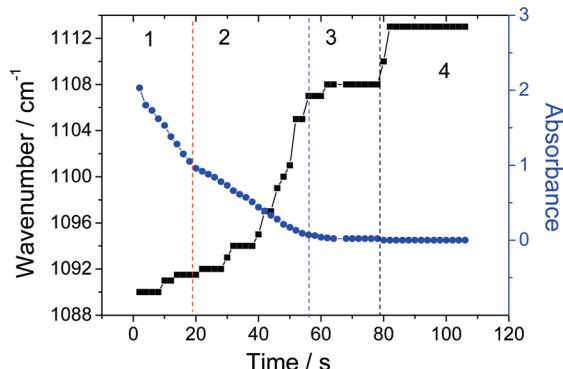


Figure 5. Intensity of the water band at 1650 cm^{-1} (right y axis) and the peak position of the 1090 cm^{-1} band as a function of time (left y axis). Numbers from 1 to 4 indicate the different evaporation stages; for details refer to the text.

the wavenumber, the y-axis represents the time scale in seconds, and the different colors denote the intensity scale of absorbance. Figure 3 gives an immediate time-resolved correlation between water evaporation and a change in the Pluronic state; we have divided the 3D spectra into four distinctive regions (*vide infra*). The water evaporation is almost complete after less than 50 s, at the same time we can observe a drastic change in the 1090 cm^{-1} band, which is indicative of the amorphous state and is perfectly time correlated with the completion of water evaporation. The same correlation can be seen in Figure 4 (left side), which shows the 3D RSTR infrared spectra of the bands in the CH_2 wagging region ($1320\text{--}1400\text{ cm}^{-1}$). The 1350 cm^{-1} band, which is indicative of the amorphous phase of Pluronic F127, disappears after 50 s and two new bands, which are due to crystalline Pluronic (*vide supra*), appear after a short time delay of 15 s.

To obtain a more quantitative correlation between water evaporation and the state transitions of the block copolymer,

we have reported in a graph (Figure 5) the intensity of the water band at 1650 cm^{-1} (right y axis) and the peak position of the 1090 cm^{-1} band as a function of time (left y axis). In particular, the change in intensity of the water band vs time gives an indication of the presence of any variation in the evaporation rate during the last part of the process. In the graph we may recognize four different evaporation rates of water, which correspond to well-defined shifts in the 1090 cm^{-1} peak wavenumber. As we have described in the previous section, a transition from an amorphous to a crystalline state is revealed in the infrared spectra by the formation of a triplet of overlapped bands in the C–O–C stretching region and the shift to higher energies of the 1090 cm^{-1} band. We have highlighted these regions in the graph and indicated them from 1 to 4, which correspond to well-defined areas that we have identified in the 3D spectra (Figures 3 and 4). These data allow getting a better clue about the phase changes of Pluronic during water evaporation; in the stage 1, water evaporates with a faster rate and the block copolymer is in its amorphous state. During this last part of the evaporation of the droplet the concentration of Pluronic F127 increases until the amount of water is low enough to give rise to a gel phase.²⁵ We tentatively assign stage 2 to the formation of a gel with the close packing of the micelles. At this point the micelles are interconnected but the presence of residual water hampers the crystallization. In stage 3, when most of the water is evaporated, we observe the beginning of an ordered phase, which is fully realized only after the complete evaporation of water (stage 4). The optical image of the droplet (Figure 6) after the end of the process shows that Pluronic F127 forms a small disk with thick borders; this is an indication of a stain effect²⁶ during evaporation that accumulates a higher amount of the block copolymer to the external side of the disk. This disk is formed of crystalline Pluronic F127 (*vide infra*) with some residual amount of disordered phase, whose presence is revealed by a small shoulder around 1080 cm^{-1} in the

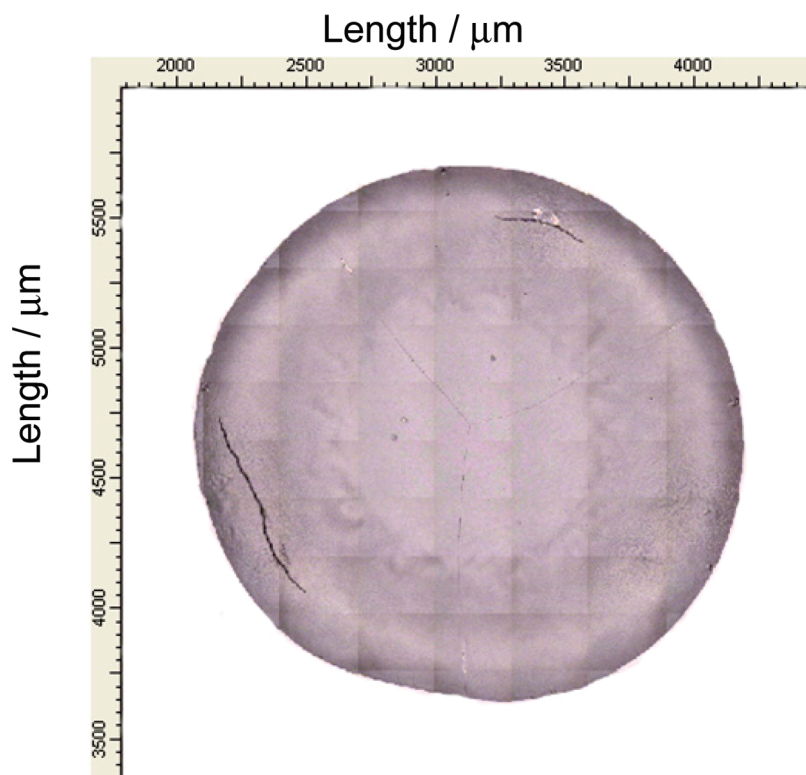


Figure 6. Optical image of the water–Pluronic F127 droplet at the end of the evaporation.

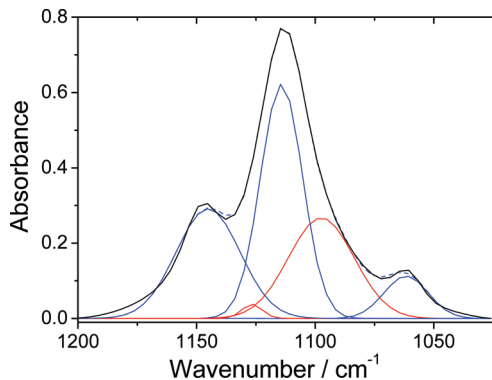


Figure 7. Deconvolution of the FTIR spectrum taken from Pluronic after the evaporation in the 1200–1025 cm⁻¹ region (black line). Five Gaussian curves are used to fit the spectrum: three components for the crystalline (blue lines) and two for the noncrystalline (red line) contributions. The fit is shown in a blue dash line.

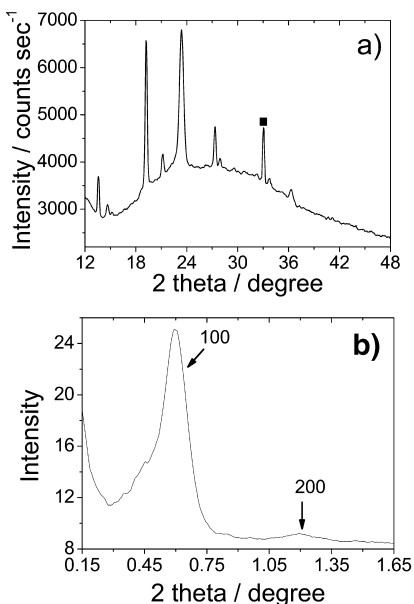


Figure 8. (a) Wide-angle XRD of the Pluronic F127 droplet after evaporation on a silicon wafer; the full black square indicates a diffraction peak due to the silicon substrate. (b) Small-angle X-ray scattering of the Pluronic F127 droplet after evaporation on a silicon wafer: the indexation of the lamellar mesophase is shown in the figure.

crystalline band at 1111 cm⁻¹ of the FTIR spectrum taken from the disk (Figure 7). We have made a deconvolution of the final spectrum in the 1200–1025 cm⁻¹ region, we have used five Gaussian curves to fit the spectrum, three components for the crystalline and two for the noncrystalline contributions. Evaluating the relative area of the Gaussian components assigned to the amorphous phase (red curves in Figure 7), we have obtained a semiquantitative evaluation of the final composition, with 28% of residual nonordered phase. We have characterized the structure of the disk formed by Pluronic F127 upon evaporation by X-ray diffraction and SAXS. The XRD patterns show the typical signature of crystalline PEO in Pluronic F127²⁷ and well support the FTIR spectrum of the final material (Figure 8a); in particular, the baseline shows a bump that is due to the amorphous part of the block copolymer supporting also in this case the FTIR data. Beside the crystallization of the PEO chains in Pluronic F127, the surfactant in the dried state self-organizes into a lamellar mesophase, as shown by the SAXS pattern (Figure 8b).

Conclusions

We have studied in situ the evaporation process of a droplet of aqueous solution containing a block copolymer, Pluronic F127, by a spectroscopic method. The technique allows reaching a temporal resolution of ~1 s suitable to study the processes involved and represents an ideal analytical tool for these types of phenomena.

The changes in the state of Pluronic F127 become dramatic at the last stage of the evaporation process and appear driven by water evaporation with the increase of Pluronic concentration. Water evaporation rate, which is almost constant during most of the process, suddenly changes in the last two minutes. This phenomenon appears correlated to well-specific transitions of the block copolymer phase, which changes from amorphous to partial crystalline state.

References and Notes

- Hadjichristidis, N.; Pispas, S.; Floudas, G. A. *Block Copolymers*; Wiley & Sons: New York, 2003.
- Lu, Y. F.; Ganguli, R.; Drewien, C. A.; Anderson, M. T.; Brinker, C. J.; Gong, W. L.; Guo, Y. X.; Soyez, H.; Dunn, B.; Huang, M. H.; Zink, J. I. *Nature* **1997**, *389*, 364.
- Alexandridis, P.; Holzwarth, J. F.; Hatton, T. A. *Macromolecules* **1994**, *27*, 2414.
- Olson, D. A.; Chen, L.; Hillmyer, M. A. *Chem. Mater.* **2008**, *20*, 869.
- Bockstaller, M. R.; Mickiewicz, R. A.; Thomas, E. L. *Adv. Mater.* **2005**, *17*, 1331.
- Brinker, C. J.; Lu, Y.; Sellinger, A.; Fan, H. *Adv. Mater.* **1999**, *7*, 11.
- Soler-Illia, G.; Innocenzi, P. *Chem.—Eur. J.* **2006**, *12*, 4478.
- (a) Huo, Q.; Margolese, D. I.; Ciesla, U.; Demuth, D. G.; Feng, P.; Gier, T. E.; Sieger, P.; Firouzi, A.; Chmelka, B. F.; Schüth, F.; Stucky, G. D. *Chem. Mater.* **1994**, *6*, 1176. (b) Soler-Illia, G. J. A. A.; Crepaldi, E. L.; Gross, D.; Sanchez, C. *Curr. Opin. Colloid Interface Sci.* **2003**, *8*, 109.
- Gross, D.; Balkenende, A. R.; Albouy, P. A.; Ayral, A.; Amenitsch, H.; Babonneau, F. *Chem. Mater.* **2001**, *13*, 1848.
- (a) Innocenzi, P.; Malfatti, L.; Kidchob, T.; Falcaro, P.; Cestelli Guidi, M.; Piccinini, M.; Marcelli, A. *Chem. Commun.* **2005**, 2385. (b) Falcaro, P.; Costacurta, S.; Mattei, G.; Amenitsch, H.; Marcelli, A.; Cestelli Guidi, M.; Piccinini, M.; Nucara, A.; Malfatti, L.; Kidchob, T.; Innocenzi, P. *J. Am. Chem. Soc.* **2005**, *127*, 3838.
- (a) Innocenzi, P.; Malfatti, L.; Kidchob, T.; Costacurta, S.; Falcaro, P.; Piccinini, M.; Marcelli, A.; Morini, P.; Salvi, D.; Amenitsch, H. *J. Phys. Chem. C* **2007**, *111*, 5345. (b) Marcelli, A.; Hampai, D.; Xu, W.; Malfatti, L.; Innocenzi, P. *Acta Phys. Pol. A* **2009**, *115*, 489.
- Innocenzi, P.; Kidchob, T.; Malfatti, L.; Costacurta, S.; Takahashi, M.; Piccinini, M.; Marcelli, A. *J. Sol-Gel Sci. Technol.* **2008**, *48*, 253.
- Innocenzi, P.; Kidchob, T.; Mio Bertolo, J.; Piccinini, M.; Cestelli Guidi, M.; Marcelli, A. *J. Phys. Chem. B* **2006**, *110*, 10837.
- Innocenzi, P.; Malfatti, L.; Piccinini, M.; Marcelli, A.; Gross, D. *J. Phys. Chem. A* **2009**, *113*, 2745.
- Innocenzi, P.; Malfatti, L.; Costacurta, S.; Kidchob, T.; Piccinini, M.; Marcelli, A. *J. Phys. Chem. A* **2008**, *112*, 6512.
- (a) Su, Y. L.; Wang, J.; Liu, H.-Z. *Macromolecules* **2002**, *35*, 6426. (b) Su, Y.-L.; Liu, H.-Z.; Guo, C.; Wang, J. *Mol. Simul.* **2003**, *29*, 803.
- Barba, A. A.; D'Amore, M.; Grassi, M.; Chirico, S.; Lamberti, G.; Titomanlio, G. *J. Appl. Polym. Sci.* **2009**, *114*, 688.
- Schmidt, P.; Dybal, J.; Sturcova, A. *Vib. Spectrosc.* **2009**, *50*, 218.
- Dissanayakket, M.; Frech, R. *Macromolecules* **1995**, *28*, 5312.
- Marcos, J. I.; Oriandi, E.; Zerbi, G. *Polymer* **1990**, *31*, 1899.
- Cabana, A.; Ait-Kadi, A.; Juhász, J. *J. Colloid Interface Sci.* **1997**, *190*, 307.
- Li, X.; Hsu, S. L. *J. Polym. Sci., Polym. Phys. Ed.* **1984**, *22*, 1331.
- Zerbi, G.; Magni, R.; Gussoni, M.; Moritz, K. H.; Bigotto, A.; Dirlikov, S. *J. Chem. Phys.* **1981**, *75*, 3175.
- Alexandridis, P.; Zhou, D.; Khan, A. *Langmuir* **1996**, *12*, 2690.
- Li, Y.; Shi, T.; Sun, Z.; An, L.; Huang, Q. *J. Phys. Chem. B* **2006**, *110*, 26424.
- Innocenzi, P.; Malfatti, L.; Piccinini, M.; Gross, D.; Marcelli, A. *Anal. Chem.* **2009**, *81*, 551.
- Lazzara, G.; Milioto, S.; Gradzielski, M.; Prevost, S. *J. Phys. Chem. C* **2009**, *113*, 12213.